Supporting Information

Reversible Removal of Intermixed Shallow States by Light Soaking in Multi-Cation Mixed Halide Perovskite Films

*Dengyang Guo[1], Zahra Andaji Garmaroudi[2], Mojtaba Abdi-Jalebi[2], Samuel D. Stranks[2], and Tom J. Savenije[1]**

[1]Department of Chemical Engineering, Delft University of Technology, 2629 HZ Delft, The Netherlands

[2]Cavendish Laboratory, JJ Thomson Avenue, Cambridge CB3 0HE, United Kingdom

AUTHOR INFORMATION

Corresponding Author

*E-mail: T.J.Savenije@tudelft.nl

Experimental Methods

Sample preparation.

Lead iodide and lead bromide were purchased from TCI, organic cations were purchased from Dyesol, and cesium iodide was obtained from Alfa Aesar. Triple-cation pure iodide $(Cs_{0.06}MA_{0.15}FA_{0.79})Pb(I)_3$ and pure bromide $(Cs_{0.06}MA_{0.15}FA_{0.79})Pb(Br)_3$ perovskite precursor solutions were prepared by using PbI_2 (1.32 M), formamidinium iodide (1.00 M), and methylammonium iodide (0.20 M) for the pure iodide solution, and $PbBr_2$ (1.32 M), formamidinium bromide (1 M), and methylammonium bromide (0.20 M) for the pure bromide solution. The precursors were dissolved in a mixture of anhydrous DMF:DMSO (4:1 volume ratio, v:v) followed by addition of 5 vol% from CsI stock solution (1.5 M in DMSO) to each solution. The series of mixed halide compositions $(Cs_{0.06}MA_{0.15}FA_{0.79})Pb\ (I_{1-x}Br_x)_3$ $0 \leq x \leq 1$ were then made from mixing the pure iodide and pure bromide solutions in different volume fractions. Quartz substrates were cleaned by sonication in acetone and isopropyl alcohol for 30 min, and further cleaning with oxygen plasma treatment for 10 min. For deposition of the perovskite solutions, we used a two-step spin-coating program at 1,000 and 4,000 rpm for 10 and 30 s respectively, and 110 μl of chlorobenzene was poured on the spinning substrate 30 s after the starting of the program. The substrates were then annealed for 1 hour at 100°C. Synthesis and deposition of perovskite solutions were performed inside a nitrogen glove box under moisture- and oxygen-controlled conditions (H_2O level: <1 ppm and O_2 level: <10 ppm).

Time-Resolved Microwave Conductivity (TRMC).

The TRMC technique monitors the change in reflected microwave power by the excited free charge-carriers in the samples loaded in a microwave open cell upon pulsed laser excitation. The illumination spot of the pulsed laser covers nearly the whole area of the sample (2 cm^2).

The photo-conductance (ΔG) of the samples was deduced from the measured laser-induced change in normalized microwave power ($\Delta P/P$) by

$$-K\Delta G(t) = \frac{\Delta P(t)}{P} \tag{1}$$

where K is the sensitivity factor. The yield of generated free charges φ and mobility $\sum\mu = (\mu_e + \mu_h)$ were obtained by:

$$\varphi\sum\mu = \frac{\Delta G}{I_0 \beta e F_A} \tag{2}$$

where, I_0 is the number of photons per pulse per unit area, β is a geometry constant of the microwave cell, e is the elementary charge, and F_A is the fraction of light absorbed by the sample at the excitation wavelength of 500 nm is 0.8.

Photoluminescence characterization.

Fluorescence spectra was measured in a Nitrogen filled chamber using a 532-nm continuous-wave laser at an illumination intensity of ~60 mW/cm^2. Light soaking of the samples was carried out by the same laser at the same intensity. We used an optical fiber coupled to an Ocean Optics Maya2000 Pro spectrometer to collect the emitted photoluminescence.

Absorption Spectra.

Absorption spectra were recorded with a Lambda 1050 UV/Vis/NIR (PerkinElmer, Inc., Shelton, CT USA) spectrophotometer, using an integrated sphere. The percentage of absorbed light was determined from the percentage of reflected light and transmitted light by the MHP films.

Photothermal Deflection Spectroscopy (PDS).

PDS is a highly sensitive surface averaged optical absorption measurement technique. PDS is capable of measuring 5-6 orders of magnitude weaker absorbance than the band edge absorption. For the measurements, a monochromatic pump light beam is shined on the sample (film on quartz substrate), which on absorption produces a thermal gradient near the sample surface via non-radiative relaxation induced heating. This results in a refractive index gradient in the area surrounding the sample surface (the sample is immersed in a Fluorinert FC-72 high refractive index gradient inert liquid). A fixed wavelength CW laser probe beam is passed through this refractive index gradient producing a deflection proportional to the absorbed light at that particular wavelength, which is detected by a photo-diode and lock-in amplifier. Scanning through different wavelengths provides a complete absorption spectrum. For PDS measurements, the perovskite films were deposited on quartz substrates and measure before and after white light treatment with the intensity of approximately 1 sun in nitrogen.

TRMC fitting equations

$$\frac{d\Delta n}{dt} = G_c - k_2 \Delta n(\Delta p + p_0) - k_T \Delta n(N_T - n_t) - k_s \Delta n + k_r n_{ts} \tag{S1}$$

$$\frac{d\Delta p}{dt} = G_c - k_2 \Delta n(\Delta p + p_0) - k_D n_t(\Delta p + p_0) \tag{S2}$$

$$\frac{dn_t}{dt} = k_T \Delta n(N_T - n_t) - k_D n_t(\Delta p + p_0) \tag{S3}$$

$$\frac{dn_{ts}}{dt} = k_s \Delta n - k_r n_{ts} \tag{S4}$$

In this set of differential equations, G_c is the optical generation of charge carriers; Δn, Δp, n_t and n_{ts} represent the concentrations of photo-excited electrons in the CB, holes in the VB, electrons trapped in deep traps, and electrons residing in shallow states, respectively; p_0

stands for the concentration of background holes, and N_T denotes the density of deep traps.

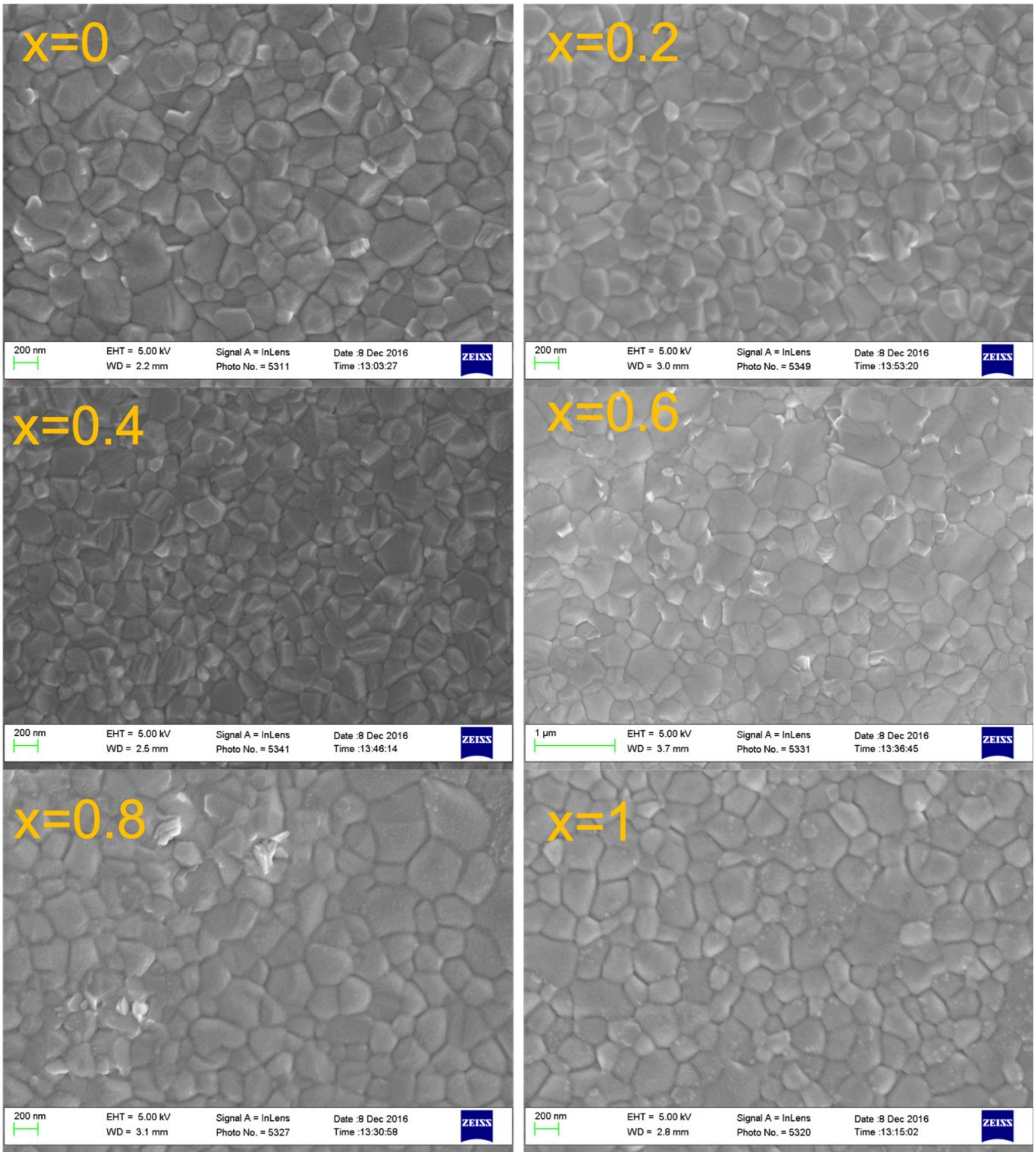

Figure S1. SEM images of $(FA_{0.79}MA_{0.16}Cs_{0.05})Pb(I_{1-x}Br_x)_3$ perovskites.

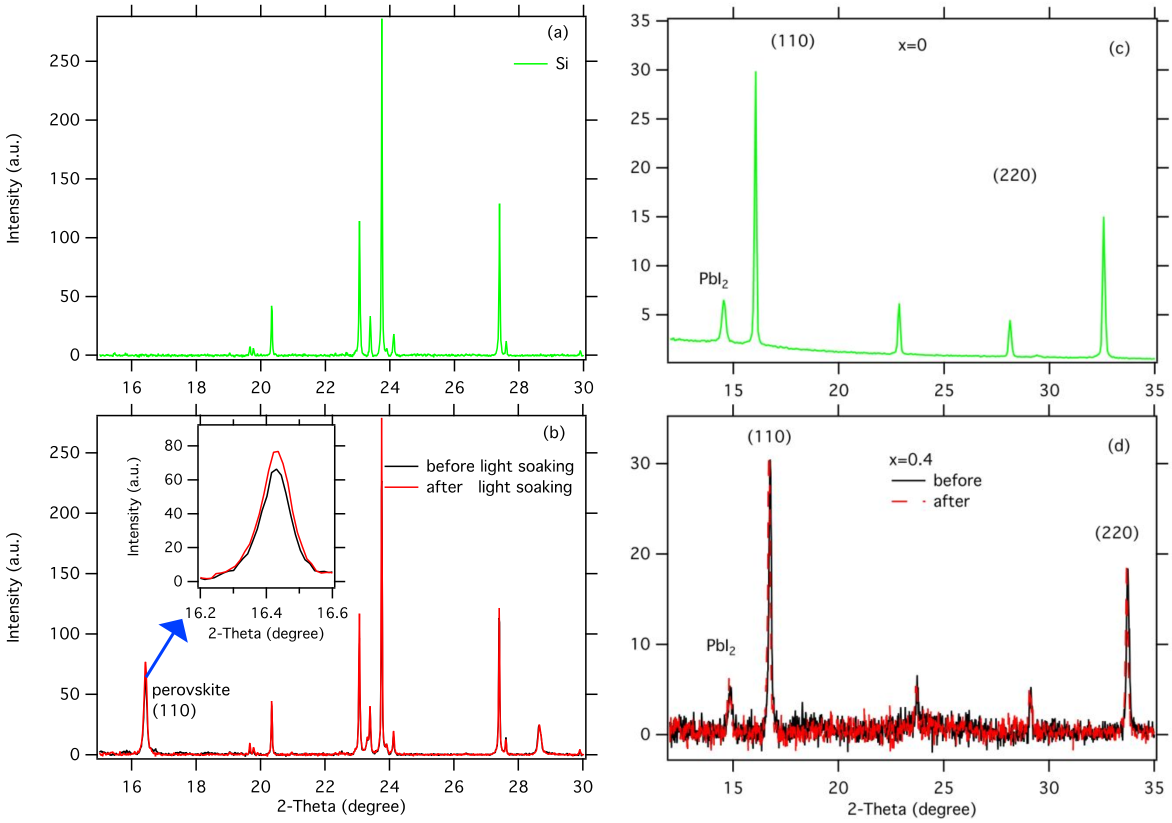

Figure S2. XRD patterns measured using a Co K$\boldsymbol{\alpha}$, $\boldsymbol{\lambda} =$ 1.79Å source. Reference Si (111) wafer (a), MCMHP with x = 0.4 before (black) and after (red) light soaking (b). The (110) diffraction peak of the perovskite is shown in the inset. Patterns for MCMHP on quartz with x = 0.0 (c) and x = 0.4 (d). For MCMHP with x = 0, a Cu K$\boldsymbol{\alpha}$ ($\boldsymbol{\lambda} =$ 1.54Å) was used, and corresponding 2$\boldsymbol{\theta}$ plot of graph (c) has been recalculated.

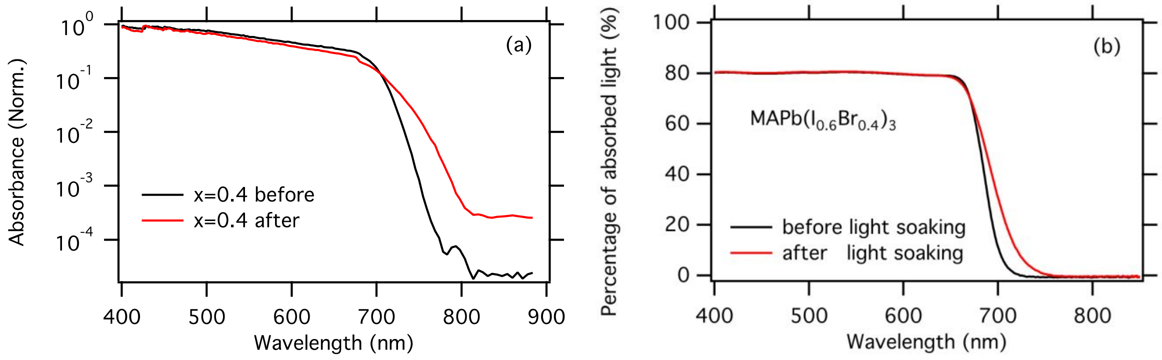

Figure S3. (a) PDS spectra of $(FA_{0.79}MA_{0.15}Cs_{0.06})Pb(I_{1-x}Br_x)_3$ with x = 0.4 before and after light soaking in N_2 (b)Percentage of absorbed light before and after light soaking in N_2 for $MAPb(I_{0.6}Br_{0.4})_3$.

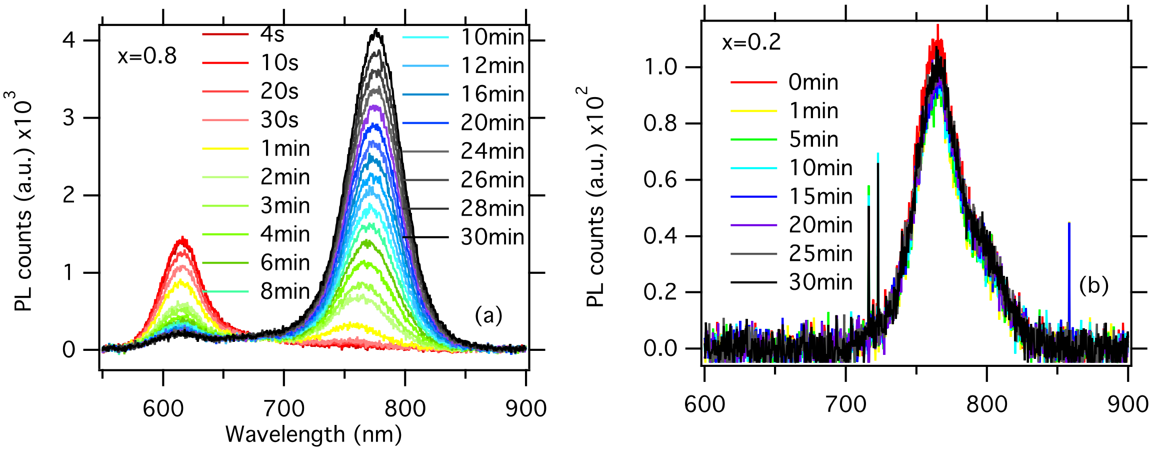

Figure S4. PL on light soaking in N_2 of the sample (a) x=0.8, and (d) x=0.2, respectively.

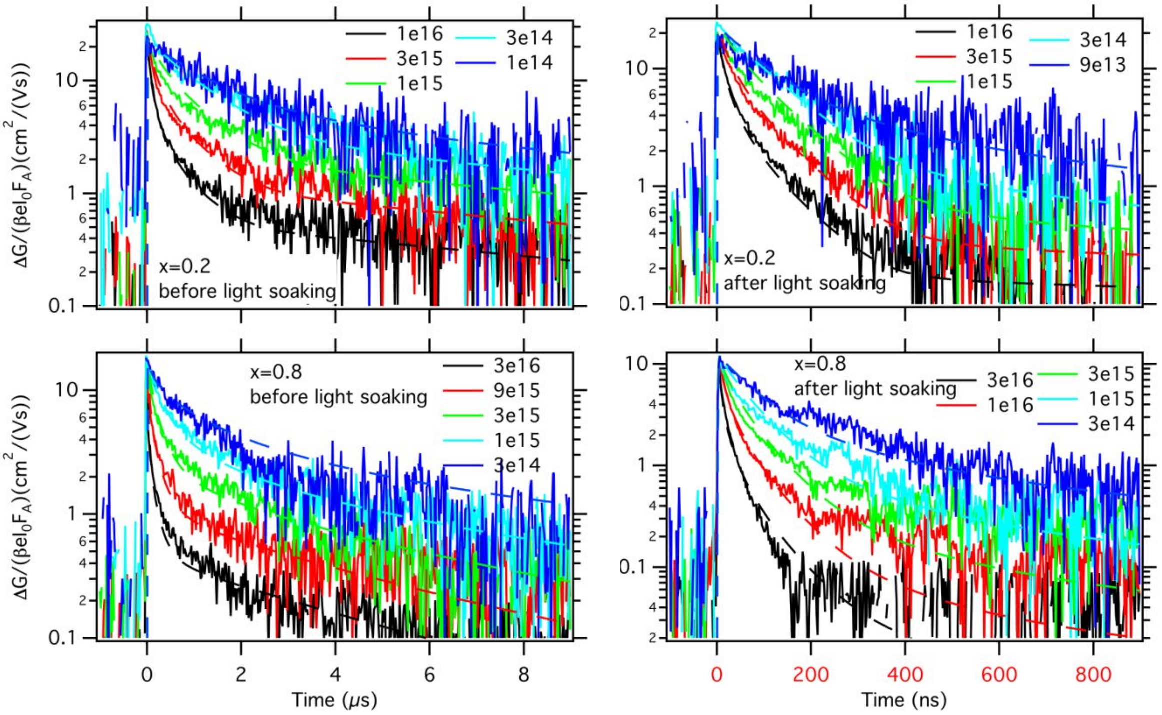

Figure S5. TRMC traces of $(FA_{0.79}MA_{0.16}Cs_{0.05})Pb(I_{1-x}Br_x)_3$ perovskites for x=0.2 and x=0.8, respectively before (left) and after (right) light soaking.

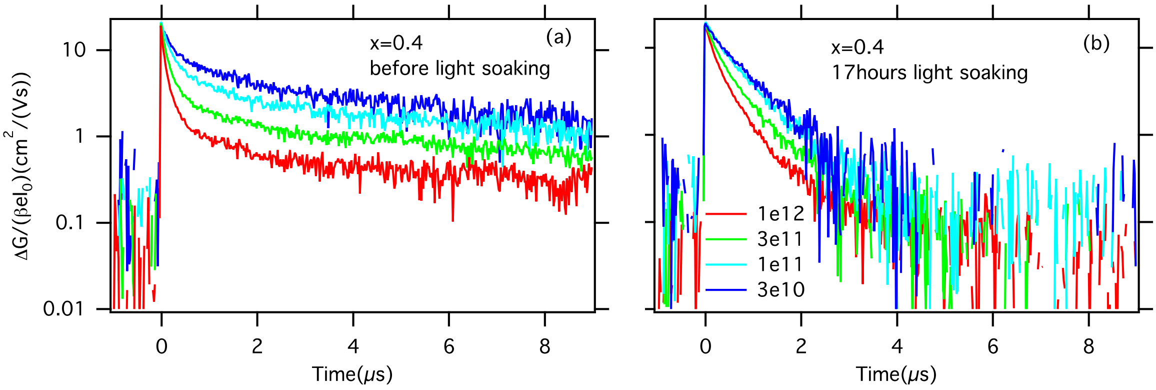

Figure S6. TRMC traces of $(FA_{0.79}MA_{0.16}Cs_{0.05})Pb(I_{0.6}Br_{0.4})_3$ before (a) and after (b) light soaking for overnight, 17 hours.

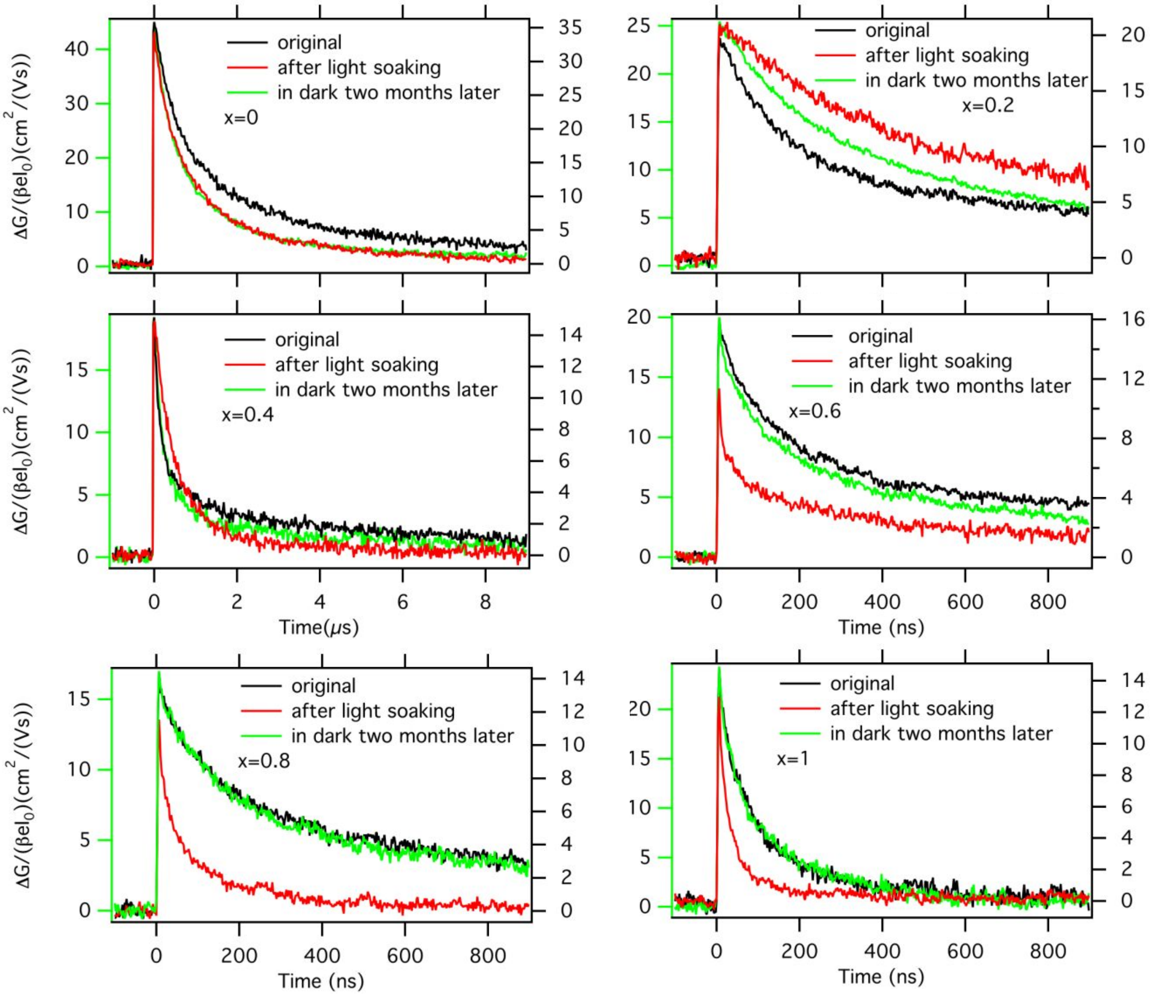

Figure S7. Recovery of samples recorded two months later, on an excitation density of 1x10^{15} cm^{-3}. The samples were kept in the dark in a N_2 glovebox.

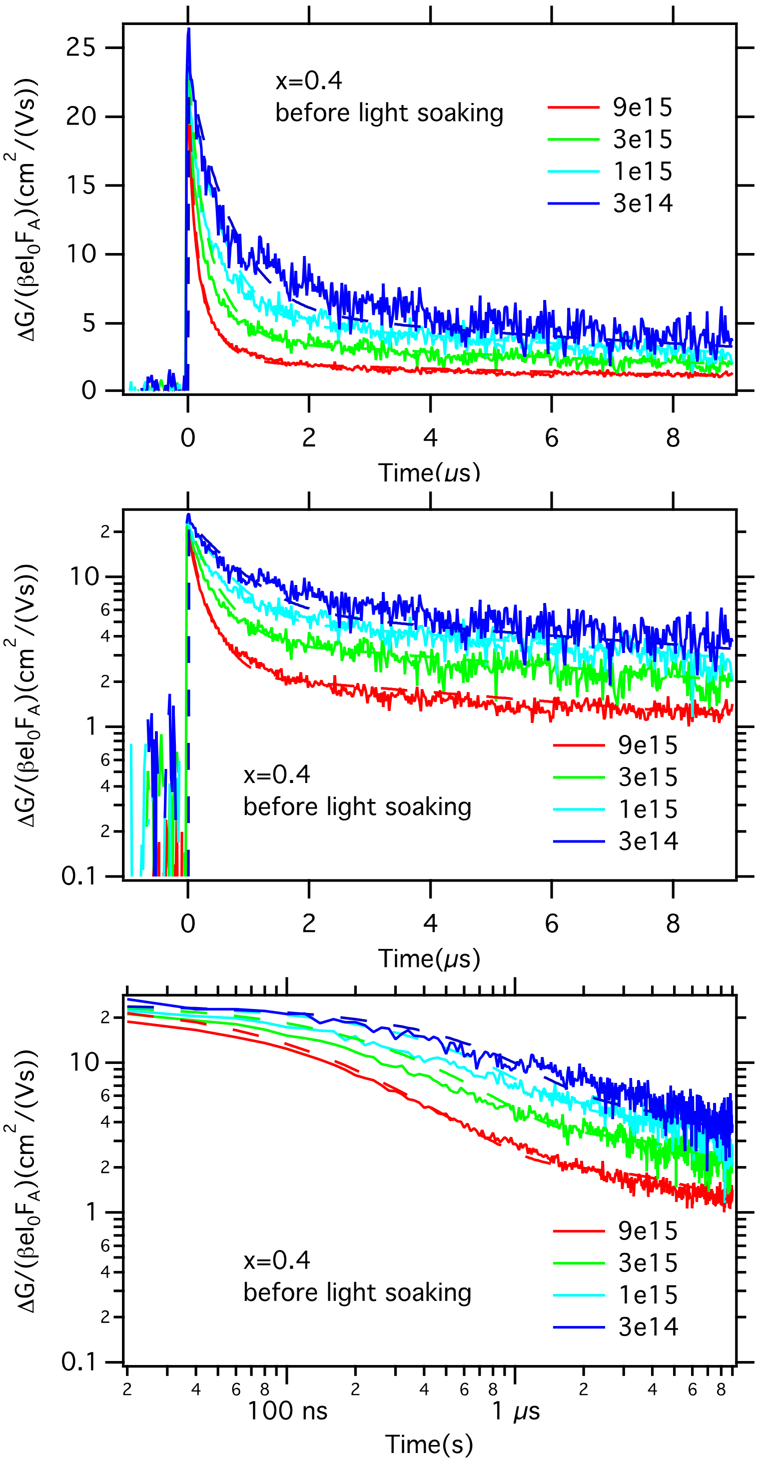

Figure S8. TRMC traces of $FA_{0.79}MA_{0.16}Cs_{0.05}Pb(I_{1-0.6}Br_{0.4})_3$ on linear-linear, logarithm-linear, and logarithm- logarithm scale, respectively. The dashed lines are the results of the fits using the model depicted in Figure 4a.

Table S1. Dynamic parameters extracted from the fitting for the samples $FA_{0.79}MA_{0.16}Cs_{0.05}Pb(I_{1-0.6}Br_{0.4})_3$ from x=0 to x=1. Those of $MAPb(I_{0.6}Br_{0.4})_3$ are also included.

Head 1 [units]	x=0		x=0.2		x=0.4		x=0.6		x=0.8		x=1		$MAPb(I_{0.6}Br_{0.4})_3$	
parameters	before	after	before	after	before	after	before	after	before	after	before	after	before	after
k_T [a]	1	1	1	1	1	1	1	1	1	1	1	1	1	1
k_2 [b]	4	8.5	15	9	8	7	20	40	25	69	30	30	35	30
k_D [c]	3.8	4	1	1.5	1.5	3	12	16	0.4	6	4	9	0.8	0.8
N_T [d]	8	11	50	50	45	48	15	15	300	300	300	300	30	120
p_0 [e]	1	1	1	1	1	1	1	1	1	1	1	1	5	50
k_s [f]	6	no	20	4	70	6	80	20	80	8	no	no	no	no
k_r [g]	0.6	no	10	3	8.5	5	15	2	30	3	no	no	no	no
μ_e [h]	22	22	12	12	12	12	10	5	10	6	11	7	2	2
μ_p [i]	44	44	24	24	24	24	20	10	20	12	22	14	5	5

[a] Deep trap filling rate ($\times 10^{-7}$ cm^3s^{-1}); [b] band-to-band recombination rate ($\times 10^{-10}$ cm^3s^{-1}); [c] Deep trap depopulation rate ($\times 10^{-8}$ cm^3s^{-1}); [d] Density of deep traps ($\times 10^{12}$ cm^{-3}); [e] background concentration of holes ($\times 10^{12}$ cm^{-3}); [f] rate of trapping into the shallow states ($\times 10^{4}$ s^{-1}); [g] rate of escaping from the shallow states($\times 10^{4}$ s^{-1}); [h] mobility of electrons ($cm^2V^{-1}s^{-1}$); [i] mobility of holes($cm^2V^{-1}s^{-1}$).

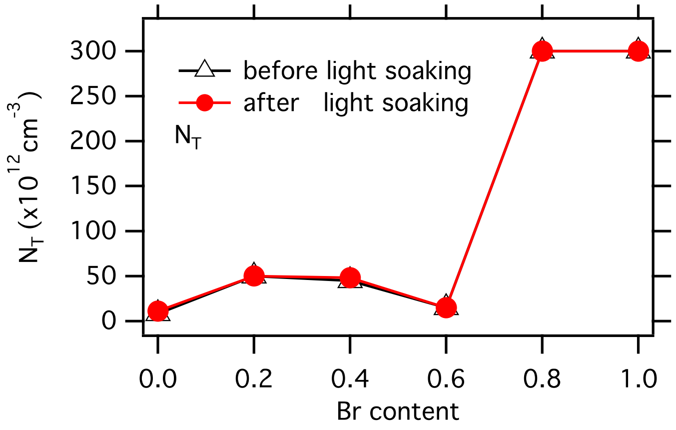

Figure S9. Density of deep trap states before (black) and after (red) light soaking, obtained from fitting.

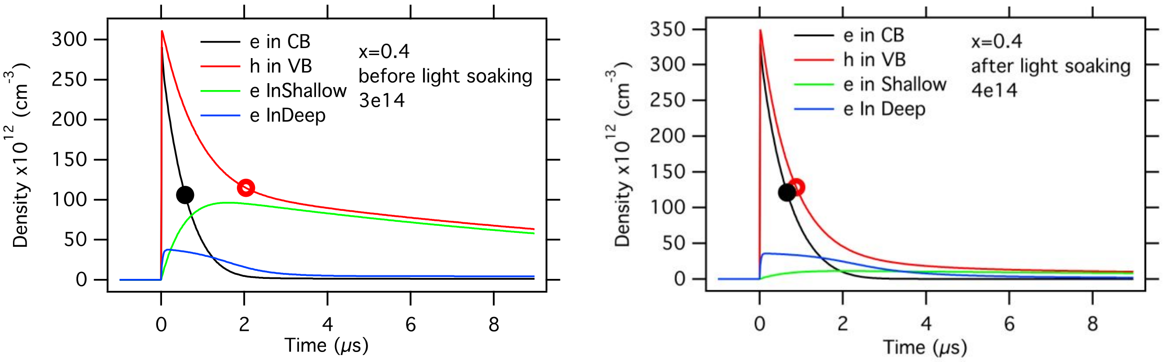

Figure S10. Decay of electrons and holes, respectively, before (left) and after (right) light soaking for x = 0.4. The excitation density is 3x10^{14} cm^{-3}. The green and blue lines show how long electrons remain in shallow and deep states, respectively. The decays are obtained by numerically solving Equations (S1 - S2) from the model. The black (red) markers denote the 1/e lifetime of electrons (holes).